Structure and Dynamics of the GABA Binding Pocket: A Narrowing Cleft that Constricts during Activation

David A. Wagner and Cynthia Czajkowski

Department of Physiology, University of Wisconsin, Madison, Wisconsin 53706

Photo-affinity labeling and mutagenesis studies have identified several amino acids that may contribute to the ligand binding domains of ligand-gated ion channels. These types of studies, however, only generate a one-dimensional, static description of binding site structure. In this study, we used the substituted cysteine accessibility method not only to identify binding pocket residues but also to elicit information about binding site dynamics and structure. Residues surrounding the putative loop C ligand binding domain of the $GABA_A$ receptor (β_2V199 to β_2S209) were individually mutated to cysteine, and the mutant subunits were coexpressed with wild-type α_1 subunits in *Xenopus* oocytes. *N*-biotinylaminoethyl methanethiosulfonate (MTSEA-biotin) reacts with cysteines introduced at positions G203, S204, Y205, P206, R207, and S209. This accessibility pattern is not consistent with either an α-helix or β-strand. Instead, G203–S209 seems to form a water-accessible extended coil, whereas V199–T202 appears to buried in the protein or membrane. Coapplication of either GABA or the competitive antagonist SR-95531 significantly slows MTSEA-biotin modification of cysteines introduced at positions S204, Y205, R207, and S209, demonstrating that these residues line and face into the GABA binding pocket. MTSEA-biotin reaction rates reveal a steep accessibility gradient from G203–S209 and suggests that the binding pocket is a deep narrowing cleft. Pentobarbital activation of the receptor significantly slows MTSEA-biotin modification of cysteines at S204, R207, and S209, suggesting that the binding site may constrict during gating.

Key words: GABA; $GABA_A$ receptor; binding site; substituted cysteine accessibility method; cysteine mutagenesis; agonist efficacy; protein structure

$GABA_A$ receptors share their fundamental structure and functional properties with an evolutionarily related superfamily of ligand-gated ion channels (LGICs) that also includes nicotinic acetylcholine (nACh), 5-HT_3, glycine, and $GABA_C$ receptors (Ortells and Lunt, 1995). For these receptors, neurotransmitter binding induces allosteric changes in the protein that result in channel opening and fast synaptic response. A complete understanding of the function of these receptors will not only require detailed structural information regarding the protein domains involved in agonist binding, transduction, and gating but will also necessitate knowledge of the relative movements of these domains, and their constituent amino acid residues, when the receptor undergoes transitions from the unliganded, closed state to the fully liganded, open state.

Although high-resolution crystal structures of liganded and unliganded receptors may ultimately help us to answer these questions, this data has proven to be notoriously elusive, and precise information regarding the structure and dynamics of the GABA binding domain remains scarce. Methods such as photo-affinity labeling and site-directed mutagenesis have led to the identification of several individual amino acid residues on the α and β subunits that may contribute to the ligand binding pocket (Sigel et al., 1992; Amin and Weiss, 1993; Smith and Olsen, 1994; Westh-Hansen et al., 1997). This work, and parallel work on the closely related nicotinic acetylcholine receptor, indicates that agonist binding takes place at inter-subunit interfaces (Czajkowski et al., 1993) and may be coordinated by residues from at least six polypeptide loops designated loop A–loop F (Corringer et al., 2000).

One means of extracting more detailed information about the secondary structure, solvent accessibility, and dynamics of a protein domain is the substituted cysteine accessibility method (SCAM) (Javitch et al., 1995; Xu and Akabas, 1996; Wilson and Karlin, 1998; Basiry et al., 1999). SCAM entails the mutation of a residue to cysteine and the subsequent observation of the functional effect (if any) caused by reaction of the introduced cysteine with a sulfhydryl reactive reagent (Karlin and Akabas, 1998). Previously, we used SCAM on the F64 region (loop D) of the $GABA_A$ α_1 subunit to define the secondary structure of this region as a β-strand and identified α_1F64, α_1R66, and α_1S68 as residues likely to line the GABA binding pocket (Boileau et al., 1999).

In the present study, we performed SCAM analysis on residues β_2V199–S209, which comprise the putative loop C domain of the GABA binding pocket. These experiments identified four residues that face into the GABA binding pocket: S204, Y205, R207, and S209. Residues that influence GABA affinity but are not part of the pocket were also identified: F200, S201, T202, and G203. Accessibility and rate of reaction studies indicate that loop C has an extended conformation that may traverse the GABA binding pocket from its rim to its depths. Finally, we demonstrate that this region of the binding pocket experiences structural rearrangements consistent with a constriction of the binding pocket during pentobarbital-mediated gating of the receptor.

Received Aug. 25, 2000; revised Oct. 10, 2000; accepted Oct. 23, 2000.

This work was supported in part by National Institute of Neurological Disorders and Stroke Grants NS10579 (to D.W.) and NS34727 (to C.C.). C.C. is a recipient of the Burroughs Welcome Fund New Investigator Award in the Basic Pharmacological Sciences. We thank Amy Kucken, Jeremy Teissére, Dr. Andrew Boileau, Dr. Meyer Jackson, and Dr. Matt Jones for critical reading of this manuscript.

Correspondence should be addressed to Dr. Cynthia Czajkowski, University of Wisconsin, Department of Physiology, Room 197 MSC, 1300 University Avenue, Madison, WI 53706. E-mail: czajkowski@physiology.wisc.edu.

		195 CCCCCCCCCCC 213
rat $GABA_A$	β_2	TKKVVFS**T**GS**Y**PRLSLSFR
	α_1	SGIVQSS**T**GE**Y**VVMTTHFL
rat nACh	α_1	Y**Y**T**CC**PDTP-**Y**LDITYHFI
rat Gly	α_1	YCT**K**H**Y**N**T**GKFTCIEARFH

Figure 1. Alignment of loop C domains from different LGICs. The β_2 loop C domain of the GABA binding site is aligned with homologous domains from the benzodiazepine binding site of the $GABA_A$ α_1 subunit, the acetylcholine binding site of the nicotinic acetylcholine receptor α_1 subunit, and the glycine binding site of the glycine receptor α_1 subunit. Residues that have been predicted to be in or near the binding pocket by photo-affinity labeling or mutagenesis are shown in *bold* (Galzi and Changeux, 1994). Residues in β_2 that were mutated to cysteines are denoted by a *C above* the wild-type residue.

MATERIALS AND METHODS

Site-directed mutagenesis. The β_2 cysteine mutant constructs were made by recombinant PCR, which has been described previously (Kucken et al., 2000). Cysteine substitutions were made in the rat β_2 subunit at positions V199, F200, S201, T202, G203, S204, Y205, P206, R207, L208, and S209 (Fig. 1). The β_2 cysteine mutants were subcloned into pGH19 (Liman et al., 1992; Robertson et al., 1996) for expression in *Xenopus laevis* oocytes. All β_2 cysteine mutants were verified by double-stranded DNA sequencing. The β_2 cysteine mutants have been named, using the single letter code, as wild-type residue, residue number, and mutated residue.

Expression in oocytes and voltage-clamp analysis. Oocytes from *Xenopus laevis* were prepared and injected with cRNA as described previously (Boileau et al., 1998). $GABA_A$ receptor rat α_1, β_2, or β_2 cysteine mutants in pGH19 were expressed by injection of cRNA into oocytes at 20 ng of each RNA species per oocyte, except for β_2-T202C, which was injected at 100 ng α_1/100 ng β_2-T202C per oocyte. RNA concentrations were determined by measuring absorbance at 260 nM and confirmed by observation of ethidium staining of RNA run out on agarose gels. The oocytes were maintained in ND96 (in mM: 96 NaCl, 2 KCl, 1 $MgCl_2$, 1.8 $CaCl_2$, and 5 HEPES, pH 7.4) supplemented with 100 μg/ml gentamicin and 100 μg/ml BSA for 2–14 d and used for electrophysiological recordings.

Oocytes under two-electrode voltage-clamp (V_{hold} of −80 mV) were perfused continuously with ND96 recording solution at a rate of 5 ml/min. The bath volume was 200 μl. Drugs and reagents were dissolved in ND96, except for *N*-biotinylaminoethyl methanethiosulfonate (MTSEA-biotin), which was made as a stock solution in DMSO and diluted to working concentrations in ND96. [DMSO] was ≤1% in final solutions and did not affect $GABA_A$ receptor properties. Standard two-electrode voltage-clamp recording was performed using a GeneClamp 500 (Axon Instruments, Foster City, CA) interfaced to a computer with a Digidata 1200 (Axon Instruments). Electrodes were filled with 3 M KCl and had a resistance of 0.5–1.5 MΩ. Data acquisition and analysis were performed using pClamp (Axon Instruments).

EC_{50} analysis. To compensate for slow drift in current responses to GABA application (I_{GABA}) and pentobarbital application ($I_{pentobarbital}$), dose–response trials were performed by applying a low concentration of agonist (EC_2–EC_7) just before the test concentration of agonist. Before curve fitting, currents evoked by each test concentration were normalized to the corresponding low-concentration current. Full dose–response curves were measured for each cell tested, and the resulting data were fit to the following equation: $I = I_{max}/(1 + (EC_{50}/[A])^n)$, where I is the peak response to a given concentration of agonist, I_{max} is the maximum current, EC_{50} is the concentration of agonist that evokes a current half the maximum, [A] is the concentration of GABA, and n is the Hill coefficient.

IC_{50} analysis. SR-95531 IC_{50} values were measured using a protocol in which an application of a fixed concentration of GABA was immediately followed by coapplication of the same concentration of GABA and a test concentration of SR-95531. For each SR-95531 concentration, inhibition was calculated as $I_{GABA\ +\ SR\text{-}95531}/I_{GABA}$. Full inhibition curves were measured for each cell tested, and the resulting data were fit to the following equation: inhibition $= 1 - 1/(1 + (IC_{50}/[Ant])^n)$, where IC_{50} is the concentration of antagonist that blocks half of I_{GABA}, [Ant] is the concentration of antagonist, and n is the Hill coefficient. K_i values were calculated using the Cheng–Prusoff/Chou equation (Cheng and Prusoff, 1973; Chou, 1974): $K_i = IC_{50}/(1 + [A]/EC_{50})$, where [A] is the concentration of GABA used, and EC_{50} is the GABA-EC_{50} for the mutant in question.

Measurement of MTSEA-biotin effects. All oocytes were tested for stability of I_{GABA} before addition of MTSEA-biotin (Toronto Research Chemicals Inc., North York, Canada) by applying a 5 sec pulse of GABA every 10 min until the peak currents varied by <3% from one trial to the next. Stability was usually obtained after three to six trials (30–60 min). GABA concentrations ranged between EC_{30} and EC_{60}. After the GABA response stabilized, we bath applied freshly diluted MTSEA-biotin (2 mM) for 2 min, washed for 5 min, and then recorded I_{GABA} at the same concentration used before MTSEA-biotin treatment. The covalent effect of MTSEA-biotin was calculated as $(I_{GABA\text{-}post}/I_{GABA\text{-}pre}) - 1$.

Rate of reaction assays. The rate at which MTSEA-biotin covalently modified introduced cysteines was determined by observing the effects of sequential applications of MTSEA-biotin on I_{GABA}. The protocol was as follows: apply GABA (EC_{30}–EC_{50}) for 5 sec, wash for 30 sec, apply MTSEA-biotin for 5–20 sec, wash for 2.5 min, and repeat sequence (see Fig. 4). This protocol was repeated until the reaction was complete (I_{GABA} no longer changed). To accommodate for the disparate rates at which MTSEA-biotin reacts with the various mutants, the concentration and time of MTSEA-biotin application was varied as follows: G203C, 1 μM, 5 sec; S204C, 1 μM, 10 sec; Y205C, 200 μM, 10 sec; P206C, 200 μM, 20 sec; R207C, 200 μM, 20 sec; and S209C, 1 mM, 10 sec. The effects of agonists and antagonists on reaction rates were assayed by coapplying GABA (EC_{60}–EC_{80}), SR-95531 (IC_{90}–IC_{95}), or pentobarbital (50 μM or 1 mM) with the MTSEA-biotin.

The data gathered with the rate of reaction protocol was plotted as I_{GABA} versus cumulative time of MTSEA-biotin exposure The pseudo-first-order rate constant (k) was determined by fitting the plotted data to a single exponential decay equation: $y = (\text{span} - \text{span} \times e^{-kt}) + \text{plateau}$, where span = max − plateau. The second-order rate constant (k_2) was determined by dividing the pseudo-first-order rate constant by the concentration of MTSEA-biotin used (Pascual and Karlin, 1998). To verify the accuracy of our protocol, k_2 was determined at two different concentrations of MTSEA-biotin for several of the mutants.

Statistical analysis. When determining EC_{50}, IC_{50}, or k_2, complete data sets were obtained from individual oocytes. Curve fitting was subsequently performed on the data from each oocyte, and the resultant parameters were used in statistical analysis. Statistical analysis for significant differences was performed by one-way ANOVA with Dunnett's *post hoc* test for multiple independent samples. In the case of EC_{50} and IC_{50} results, analysis for significance was performed using log values. All curve fits and statistical analysis were performed using Prism software (GraphPad Software Inc., San Diego, CA).

RESULTS

Cysteine mutation of the β_2 loop C region

Mutations at β_2-Y205 and β_2-T202 cause large shifts in $EC_{50\text{-}GABA}$ values of $\alpha_1\beta_{2mut}$ and $\alpha_1\beta_{2mut}\gamma_2$ $GABA_A$ receptors but have no effect on direct activation of receptors by pentobarbital (Amin and Weiss, 1993), indicating that these residues may contribute to the ligand binding pocket. These residues align with putative ligand binding domains of the nACh α subunit (Dennis et al., 1988) and the glycine receptor α subunit (Vandenberg et al., 1992), and this region has been termed loop C (Corringer et al., 2000). To fully evaluate the contribution of the loop C region to ligand binding and gating in the $GABA_A$ receptor, 11 cysteine mutants were made at positions V199, F200, S201, T202, G203, S204, Y205, P206, R207, L208, and S209 of the β_2 subunit (Fig. 1). The mutant β_2 subunits were then coexpressed with wild-type α_1 subunits in *Xenopus* oocytes and physiologically characterized using the two-electrode voltage-clamp technique.

All of the mutant subunits assembled into functional $\alpha_1\beta_{2mut}$ receptors. Mean maximal responses to GABA ranged from 1 to 10 μA and did not differ significantly from wild type (data not shown). GABA dose–response analysis of the mutant receptors revealed six residues that cause shifts in $EC_{50\text{-}GABA}$ values when mutated to cysteine, demonstrating that $EC_{50\text{-}GABA}$ is exquisitely sensitive to perturbation of this domain. The F200C, S201C, or

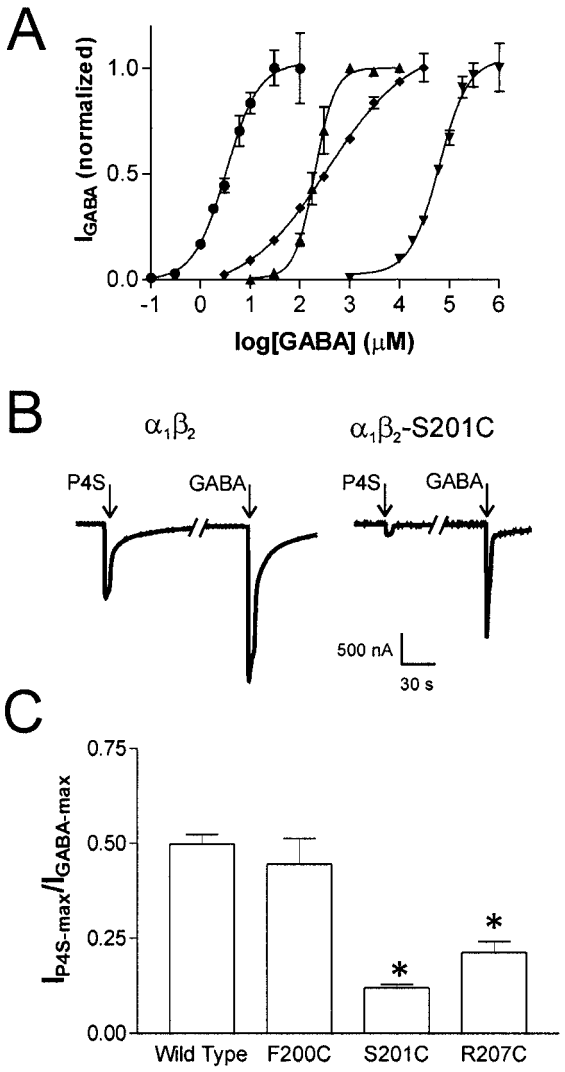

Figure 2. GABA dose–response curves and P4S currents. *A*, GABA dose–response relationships for wild-type $\alpha_1\beta_2$ receptors (●) and three representative mutants: $\alpha_1\beta_2$-R207C (▲), $\alpha_1\beta_2$-S201C (♦), and $\alpha_1\beta_2$-Y205C (▼). Data were fit by nonlinear regression as described in Materials and Methods. All data points are normalized to $I_{max\text{-}GABA}$ and are shown as mean responses ± SEM from four or more cells. *B*, Current traces recorded from oocytes expressing wild type or $\alpha_1\beta_2$-S201C. *Arrows* indicate a 5 sec application of saturating P4S (wild type, 1 mM; S201C, 10 mM) or GABA (wild type, 1 mM; S201C, 100 mM). *Line break* in current trace represents 5 min wash with ND96. *C*, Bar graph denoting P4S efficacy of wild-type and mutant receptors as $I_{max\text{-}P4S}/I_{max\text{-}GABA}$ where values given as mean ± SEM follow: $\alpha_1\beta_2$, 0.50 ± 0.03, $n = 4$; $\alpha_1\beta_2$-F200C, 0.45 ± 0.06, $n = 4$; $\alpha_1\beta_2$-S201C, 0.12 ± 0.01, $n = 3$; and $\alpha_1\beta_2$-R207C, 0.21 ± 0.02, $n = 4$. * $p < 0.01$ indicates values that are significantly different from wild type calculated using a one-way ANOVA with a Dunnett's *post hoc* test.

R207C mutations caused 70- to 300-fold shifts in $EC_{50\text{-}GABA}$ values relative to wild type, whereas the T202C, G203C, and Y205C mutations resulted in 4800-to 18,000-fold increases in $EC_{50\text{-}GABA}$ values (Fig. 2*A*, Table 1). All of these mutations (with the exception of R207C) also caused significant shifts in the IC_{50} values of the competitive antagonist SR-95531 (12- to 100-fold increases), but none of the mutations had a significant effect on the EC_{50} values for direct activation of the receptor by pentobarbital (Table 1). Notably, the mutations that reduced $EC_{50\text{-}GABA}$ have much smaller effects on the apparent affinity of SR-95531. This could be attributable to the fact that SR-95531, a much larger molecule than GABA, may enjoy extra binding interactions that make it more tolerant to a single point mutation within the binding pocket.

Determining agonist efficacy in cysteine mutants

Receptor occupancy and gating of LGICs can be most simply described by the model represented in Scheme 1 (del Castillo and Katz, 1957).

$$A + R \underset{}{\overset{K_{D1}}{\rightleftharpoons}} A + AR \overset{K_{D2}}{\rightleftharpoons} A_2R \overset{E}{\rightleftharpoons} A_2R^*$$

In this model, the microscopic affinity for agonist is represented by the dissociation constant (K_D) and agonist efficacy is represented by E, where E is the ratio of the number of fully liganded receptors that are open to the number of fully liganded receptors that are closed (Colquhoun, 1998). When using highly efficacious agonists ($E > 10$), changes in efficacy have little effect on maximum current and can be difficult or impossible to detect. For instance, if using an agonist with $E = 20$, a mutation that causes a twofold reduction of efficacy will only produce a 5% change in I_{max}. To determine whether the cysteine mutations that shift $EC_{50\text{-}GABA}$ also cause shifts in efficacy, experiments were performed using piperidine-sulfonic acid (P4S), which acts as a partial agonist ($E \approx 1$) at α_1 containing $GABA_A$ receptors (Krogsgaard-Larsen et al., 1980; O'Shea et al., 2000).

In oocytes expressing wild-type $\alpha_1\beta_2$ receptors, the ratio of current elicited by a saturating concentration of P4S to current elicited by a saturating GABA concentration ($I_{max\text{-}P4S}/I_{max\text{-}GABA}$) was 0.50 (Fig. 2*B*,*C*). In oocytes expressing $\alpha_1\beta_2$-F200C receptors, the $I_{max\text{-}P4S}/I_{max\text{-}GABA}$ ratio (0.45) was not significantly different from wild type, indicating that this mutation has no effect on agonist efficacy. However, oocytes expressing $\alpha_1\beta_2$-S201C and $\alpha_1\beta_2$-R207C receptors had significantly reduced $I_{max\text{-}P4S}/I_{max\text{-}GABA}$ ratios of 0.12 and 0.20, respectively (Fig. 2*B*,*C*). These results demonstrate that mutation of either β_2-S201 or β_2-R207 to cysteine reduces agonist efficacy at the GABA binding site. A reduction in efficacy can also result in a reduction of the Hill coefficient (Colquhoun, 1998) and may explain why $\alpha_1\beta_2$-S201C receptors have a significantly reduced Hill coefficient (n_H) for GABA (Fig. 2*A*, Table 1). It was not possible to test the remaining mutants that caused $EC_{50\text{-}GABA}$ shifts (T202C, G203C, and Y205C) for changes in efficacy because their severely reduced affinities require concentrations of GABA near or above 1 M to elicit maximal responses.

Reaction of introduced cysteines with MTSEA-biotin

One of the caveats of SCAM analysis is that the data gathered describes the structure of a mutant receptor that may not be the same as the structure of a wild-type receptor. Because of this, the results of SCAM studies are most reliable if the introduced mutations do not cause large changes in the functional properties of the receptor. Unfortunately, in domains that are functionally significant, even small changes in structure can translate into noticeable changes in receptor behavior. This seems to be the case for the region in question (β2V199–S209) in which 6 of the 11 mutations caused significant changes in $EC_{50\text{-}GABA}$ values. However, the fact that none of the mutations significantly affected direct activation by pentobarbital and no significant difference in $I_{max\text{-}GABA}$ was detectable suggests that the global structure of the receptor was not altered by any of the cysteine mutations, and it

Table 1. Apparent affinites of wild-type and mutant receptors for GABA, SR-95531, and pentobarbital

	GABA				SR-95531			PB		
Receptor	EC_{50} (μM)	n_H	n	wt/mut	K_i (μM)	n	wt/mut	EC_{50} (μM)	n	wt/mut
$\alpha_1\beta_2$ Wild type	4.3 ± 1.2	1.1	8	1.0	0.12 ± 0.02	8	1.0	570 ± 66	5	1.0
$\alpha_1\beta_2$-V199C	3.1 ± 0.4	1.4	4	0.7	0.08 ± 0.01	3	0.6	577 ± 195	5	1.0
$\alpha_1\beta_2$-F200C	1292 ± 170*	1.1	4	300	4.34 ± 2.6*	3	36.2	712 ± 96	3	1.2
$\alpha_1\beta_2$-S201C	725 ± 160*	0.5*	4	170	1.42 ± 0.3*	3	11.8	1038 ± 425	3	1.8
$\alpha_1\beta_2$-T202C	61100 ± 10900*	1.0	5	14000	1.90 ± 0.4*	3	15.8	690 ± 170	3	1.2
$\alpha_1\beta_2$-G203C	20480 ± 6990*	1.0	10	4800	4.67 ± 0.4*	4	38.9	1088 ± 70	3	1.9
$\alpha_1\beta_2$-S204C	1.5 ± 0.3	1.1	6	0.3	0.05 ± 0.03	5	0.4	427 ± 86	5	0.7
$\alpha_1\beta_2$Y205C	78000 ± 7070*	1.4	5	18000	12.40 ± 1.5*	3	103.3	800 ± 42	4	1.4
$\alpha_1\beta_2$-P206C	2.6 ± 1.0	1.2	4	0.6	0.53 ± 0.13	6	4.4	347 ± 46	4	0.6
$\alpha_1\beta_2$-R207C	310 ± 30*	1.3	4	70	0.11 ± 0.02	4	0.9	480 ± 72	4	0.8
$\alpha_1\beta_2$-L208C	2.7 ± 0.5	1.5	5	0.6	0.07 ± 0.02	3	0.6	327 ± 77	5	0.6
$\alpha_1\beta_2$-S209C	5.4 ± 1.1	1.1	3	1.3	0.11 ± 0.01	3	0.9	583 ± 105	3	1.0

EC_{50} and K_i values are presented as mean ± SEM. An asterisk indicates that the value is significantly different from wild type ($p < 0.01$). PB, Pentobarbital; wt, wild type; mut, mutant.

is likely that the changes in $EC_{50\text{-}GABA}$ represent small local effects. In addition, cysteine substitution of five of the residues mutated had no discernable effect on any of the receptor properties that we assayed, making them ideal candidates for this study.

Reaction of wild-type $\alpha_1\beta_2$ $GABA_A$ receptors with the sulfhydryl-specific reagent MTSEA-biotin caused no significant change in GABA-mediated current (Fig. 3). Therefore, if MTSEA-biotin treatment alters I_{GABA} in a mutant receptor, we assume that MTSEA-biotin has modified the introduced cysteine. MTSEA-biotin treatment significantly decreased I_{GABA} in 6 of the 11 mutant receptors tested (Fig. 3). For each affected mutant, I_{GABA} was inhibited as follows: G203C, −36 ± 9%; S204C, −26 ± 5%; Y205C, −98 ± 1%; P206C, −47 ± 13%; R207C, −55 ± 8%; S209C, −85 ± 1% (mean ± SEM; % inhibition = 100 × [(I_{GABA}-post MTSEA-biotin/I_{GABA}-pre MTSEA-biotin) − 1]). Because six of the seven consecutive residues from G203–S209 reacted with MTSEA-biotin, the accessibility pattern of this region is not predictive of an α-helix or β-strand and, therefore, the region is likely to be a turn or random coil. MTSEA-biotin treatment had no significant effect on I_{GABA} from V199C-, F200C-, S201C-, T202C-, and L208C-containing receptors. Because we cannot detect reaction of MTSEA-biotin with any residue from V199C to T202C, it seems likely that this region is buried in the hydrophobic core of the subunit, but it is also possible that these residues react with MTSEA-biotin without affecting I_{GABA}.

Observation of reaction of an introduced sulfhydryl with a methanethiolsulfonate (MTS) reagent can also provide information about the dimensions of the binding site crevice. MTSEA-biotin is composed of two distinct structural domains: a flexible tail ~14 Å long and 2.5 Å in diameter, and a 4 × 5 Å planar head group. The reactive disulfide is near the end of the tail, ~12 Å from the head group. Therefore, any residue that reacts with MTSEA-biotin must be accessible via an aqueous pathway >2.5 Å in diameter and <12 Å deep. GABA is a linear molecule ~6 Å long and 3 Å in diameter, and the dimensions of SR-95531 are ~16 Å long and 6 Å in diameter.

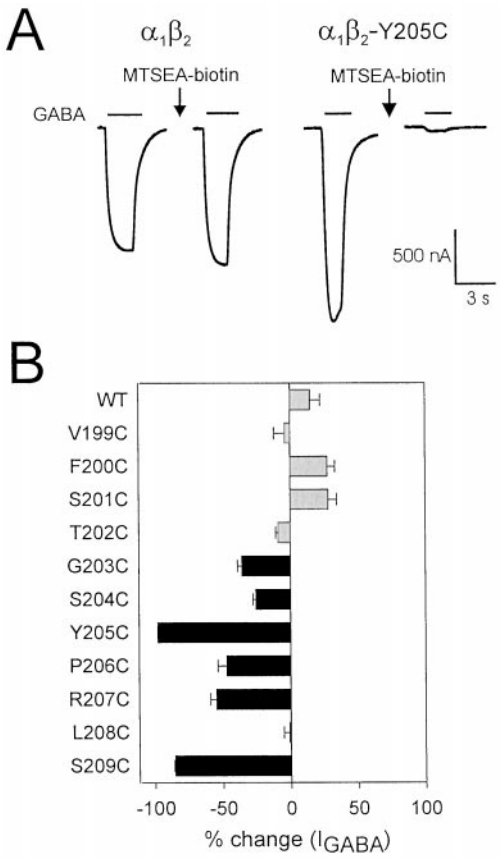

Figure 3. Effects of MTSEA-biotin on wild-type and mutant $GABA_A$ receptors. *A*, Representative current traces demonstrating the effect of MTSEA-biotin treatment (2 mM, 2 min) on currents from wild-type and Y205C-containing receptors. For wild-type traces, [GABA] is 3 μM, and for Y205C traces, [GABA] is 30 mM. *B*, Effect of MTSEA-biotin treatment on all mutants shown as % change = ([$I_{GABA\text{-post MTSEA-biotin}}$/$I_{GABA\text{-pre MTSEA-biotin}}$] − 1) × 100. Results represent the mean ± SEM of at least three experiments. *Black bars* indicate that the percent change is significantly different from wild type ($p < 0.01$). *Gray bars* indicate no significant difference from wild type ($p > 0.05$).

Measurement of MTSEA-biotin reaction rates

The rate at which MTSEA-biotin reacts with a cysteine side chain is determined by the physical environment of the sulfhydryl group (e.g., steric hindrance to reaction) and the ionization of the sulfhydryl group, which depends on the local dielectric constant and the local electrostatic potential. Thus, a residue in a relatively open, aqueous environment will display a faster rate of reaction than a

residue in a relatively restrictive, nonpolar environment (Pascual and Karlin, 1998). To acquire insight into the physicochemical environment of the loop C domain of the GABA binding site, we determined the reaction rate of MTSEA-biotin with each of the accessible introduced cysteines (G203C–R207C and S209C).

Reaction rates were measured by serial presentations of a GABA test pulse (EC_{30}–EC_{60}), followed by a 5–20 sec application of MTSEA-biotin. This protocol was repeated until I_{GABA} plateaued, and the data were plotted as I_{GABA} versus cumulative time of exposure to MTSEA-biotin. Single exponential decay curves were fit to the data, and second-order rate constants (k_2) for MTSEA-biotin were calculated (Fig. 4*A*; see Materials and Methods). The measured k_2 values span three orders of magnitude (Table 2). The fastest reaction rate was recorded for the most N-terminal residue tested (G203C, 258,000 M^{-1} s^{-1}), and the rates steadily declined with slowest reaction rate recorded at the most C-terminal residue tested (S209C, 120 M^{-1} s^{-1}). This steep rate gradient implies that this stretch of amino acids starts in a region in which the sulfhydryl group is in an aqueous environment that is highly accessible to MTSEA-biotin and steadily progresses into a much less accessible cleft.

Identification of binding site residues

To identify residues in loop C that line the GABA binding pocket, we measured the second-order rate constant (k_2) for reaction of MTSEA-biotin with each accessible introduced cysteine both in the presence of GABA and in the presence of SR-95531. SR-95531, a classical competitive agonist for GABA, binds within the GABA binding pocket. Although evidence suggests that SR-95531 may also allosterically modulate the $GABA_A$ receptor (Uchida et al., 1996; Ueno et al., 1997), it does not activate the receptor and clearly does not induce the same change in receptor structure as GABA. Therefore, if the rate at which MTSEA-biotin reacts with an introduced cysteine is slowed by both SR-95531 and GABA, then it is likely that both compounds are sterically interfering with the reaction and that the sulfhydryl side chain is facing into the GABA binding pocket. GABA (at EC_{60}–EC_{80} concentrations) and SR-95531 (at IC_{90}–IC_{95} concentrations) significantly slowed the reaction rate of MTSEA-biotin with cysteines introduced at positions S204, Y205, R207, and S209 (Fig. 5, Table 2). Therefore, these residues face into the GABA binding pocket.

State-dependent changes of binding site conformation

According to Scheme 1, receptor activation has two distinct steps, binding of agonist and isomerization of the receptor from the closed to open state. The closed-to-open transition involves a global allosteric rearrangement of the receptor that not only opens a gate but also changes the structure of the binding pocket. We examined gating-related structural changes of the GABA binding pocket by measuring the effect of the barbiturate pentobarbital on k_2 values for the MTSEA-biotin reaction.

Pentobarbital directly activates the $GABA_A$ receptor but does not bind at the same location as GABA (Ito et al., 1996). Because the single channel conductances of $GABA_A$ receptors activated by GABA and pentobarbital are similar (Jackson et al., 1982; Akk and Steinbach, 2000), it is likely that the open states of receptors activated by either of these compounds have similar conformations. Therefore, if the rate at which MTSEA-biotin reacts with an introduced cysteine is altered in the presence of pentobarbital, we infer a gating-related structural rearrangement of the binding pocket. Pentobarbital at EC_{50}–EC_{70} significantly slowed the reaction rate of MTSEA-biotin with cysteines at positions S204, R207, and S209 and significantly increased the rate at position G203 (Fig. 5, Table 2).

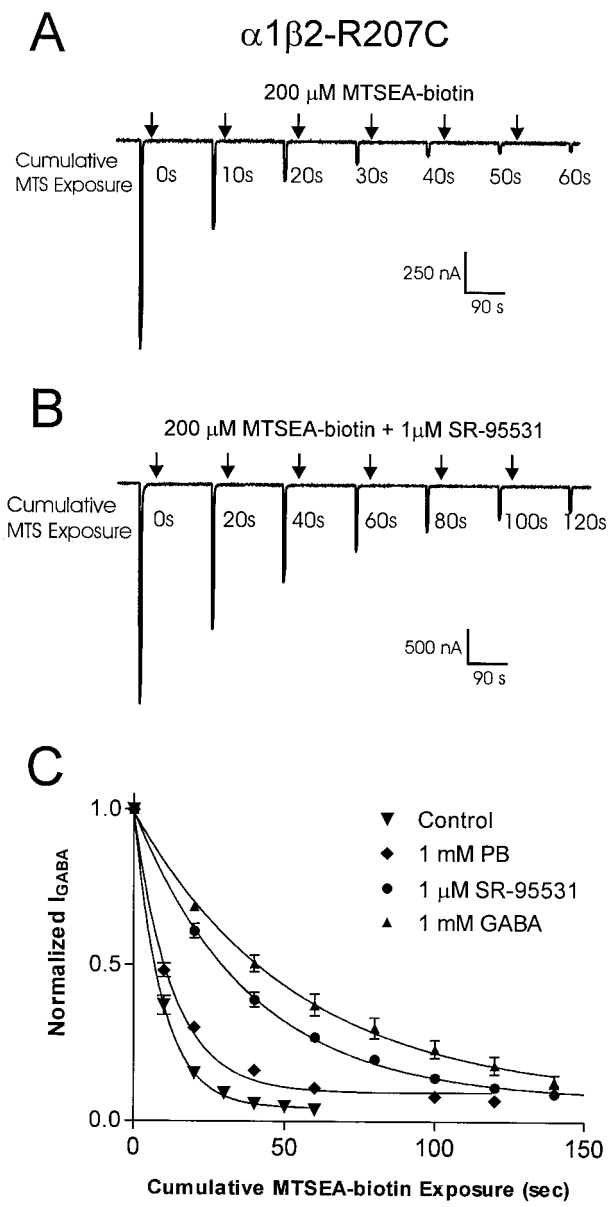

Figure 4. Measurement of MTSEA-biotin reaction rates. *A*, *B*, Examples of traces recorded during experiments measuring the reaction rate of MTSEA-biotin with $\alpha_1\beta_2$-R207C receptors. *Downward deflections* represent inward current elicited by a 5 sec application of 300 μM GABA (≈EC_{50}). *Arrows* indicate either 10 sec application of 200 μM MTSEA-biotin (*A*) or a 20 sec coapplication of MTSEA-biotin plus 1 μM SR-95531 (*B*). *C*, Normalized I_{GABA} plotted as a function of cumulative time of MTSEA-biotin exposure. Single exponential curve fits illustrate the effect of various compounds on the reaction rate of MTSEA-biotin with $\alpha_1\beta_2$-R207C receptors. Data points are normalized to the current measured at $t = 0$ and are presented as mean ± SEM. PB, Pentobarbital.

In addition to directly activating the $GABA_A$ receptor, pentobarbital potentiates GABA currents by binding to a site that is presumably separate from the site responsible for direct activation (Ito et al., 1996). Because the allosteric modulatory site has a higher apparent affinity for pentobarbital than the direct activation site (Thompson et al., 1996), rate changes induced by 1 mM pentobarbital could be attributable to its action at either of these

Table 2. Summary of second-order rate constants for reaction of MTSEA-biotin with introduced sufhydryls

	Control		GABA		SR-95531		1 mM PB		50 μM PB	
Receptor	k_2 ($M^{-1}s^{-1}$)	n	k_2 ($M^{-1}s^{-1}$)	n	k_2 ($M^{-1}s^{-1}$)	n	k_2 ($M^{-1}s^{-1}$)	n	k_2 ($M^{-1}s^{-1}$)	n
$\alpha_1\beta_2$-G203C	257,600 ± 32,700	3	184,400 ± 14,300	3	317,700 ± 19,500	3	579,200 ± 9900*	3	400,100 ± 7300*	3
$\alpha_1\beta_2$-S204C	12,060 ± 980	5	6050 ± 980*	5	3735 ± 310*	3	5656 ± 1180*	3	14,990 ± 3300	3
$\alpha_1\beta_2$-Y205C	955 ± 150	5	410 ± 15*	4	285 ± 5*	3	870 ± 40	3	ND	0
$\alpha_1\beta_2$-P206C	276 ± 41	4	715 ± 70*	3	398 ± 16	3	385 ± 25	3	352 ± 17	3
$\alpha_1\beta_2$-R207C	585 ± 40	6	100 ± 9*	4	135 ± 10*	3	370 ± 32*	3	690 ± 65	3
$\alpha_1\beta_2$-S209C	120 ± 2	4	67 ± 11*	4	40 ± 7*	3	77 ± 8*	3	125 ± 3	3

Second-order rate constants (k_2) were calculated by dividing psuedo-first-order rate constants (k_1; see Materials and Methods) by the concentration of MTSEA-biotin used during rate experiments, which were as follows: G203C, 1 μM; S204C, 10 μM; Y205C, P206C, and R207C, 200 μM; and S209C, 1 mM. Concentrations of GABA and SR-95531 present during the MTSEA-biotin reaction, which varied according to the affinity of the mutant receptor for each compound, were always between EC_{60}–IC_{80} for GABA and IC_{90}–IC_{95} for SR-95531. An asterisk indicates that the rate is significantly different from control ($p < 0.01$). PB, Pentobarbital; ND, not determined. Values are mean ± SEM.

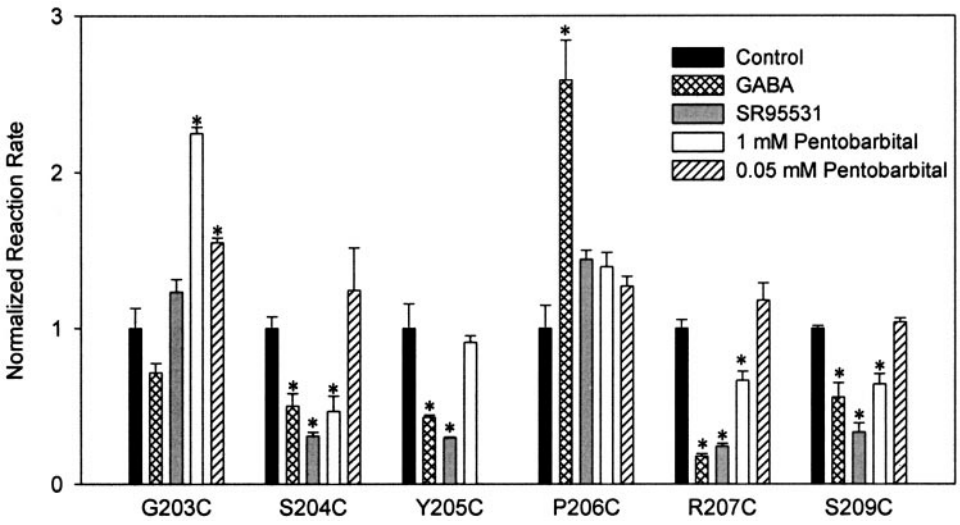

Figure 5. Summary of effect of GABA, SR-95531, and pentobarbital on the rate at which MTSEA-biotin modifies introduced cysteines. Second-order rate constants were calculated for each reaction, and for each mutant, the rates were normalized to the control rate (rate measured when no other compound is present). *$p < 0.01$ indicates that rate is significantly different from control rate. All data represent the mean ± SEM of at least three experiments.

sites. To determine whether pentobarbital effects on the MTSEA-biotin reaction rates were mediated by the high-affinity modulatory site, we measured the reaction rate in the presence of 50 μM pentobarbital, a concentration that robustly potentiates I_{GABA} but causes little direct activation of the receptor. Pentobarbital (50 μM) had no effect on the MTSEA-biotin reaction with cysteines introduced at positions S204, R207, and S209 (Fig. 5, Table 2). This result confirms the hypothesis that the ability of 1 mM pentobarbital to decrease the MTSEA-biotin k_2 values at these positions is attributable to activation of the receptor. Therefore, these residues, which we have demonstrated to be facing into the binding pocket, undergo a change in environment during gating.

The only reaction rate that was affected by a modulatory concentration of pentobarbital was for G203C, in which 50 μM pentobarbital caused an increase in k_2 (Fig. 5, Table 2). This is direct evidence that allosteric modulation of I_{GABA} by pentobarbital involves a structural rearrangement near the GABA binding pocket that makes G203C more accessible.

The rate of reaction of MTSEA-biotin with a cysteine introduced at position P206 was significantly increased in the presence of GABA. Pentobarbital and SR-95531 had no significant effect on k_2 for MTSEA-biotin at P206C (Fig. 5, Table 2). An increase in reaction rate can be interpreted as GABA binding resulting in an allosteric response that causes P206C to be in a more accessible environment. Because pentobarbital has no effect on the rate of reaction at this position, this allosteric response must be specific to rearrangements concomitant with GABA binding.

DISCUSSION

SCAM analysis of the β_2V199–S209 (loop C) region of $GABA_A$ receptor identified several amino acid residues that face into the GABA binding pocket and mediate agonist affinity (K_D) and efficacy. In addition, we provide evidence that the ligand binding pocket is a deep narrowing structure that constricts during gating.

Mutations that affect $K_{D\text{-}GABA}$

Mutation to cysteine causes significant shifts in $EC_{50\text{-}GABA}$ for six residues: F200C, S201C, T202C, G203C, Y205C, and R207C. According to the model shown in Scheme 1, shifts in $EC_{50\text{-}GABA}$ can be caused by changes in affinity of the closed receptor for GABA (K_D) and/or changes in the ability of GABA to induce opening of the receptor (efficacy or E). Determining which of these parameters is responsible for mutation-induced EC_{50} shifts is difficult (Colquhoun, 1998). However, for receptors that require the binding of two ligands for efficient opening and have relatively low E values, a large increase in EC_{50} that is not accompanied by a significant reduction in I_{max} can be attributed to a reduction in K_D (Amin and Weiss, 1993; Anson et al., 1998). In fact, for the $GABA_A$ receptor, a 50-fold increase in $EC_{50\text{-}GABA}$ would have to be accompanied by a >99% reduction in $I_{max\text{-}GABA}$ for the shift in the dose–response curve to be caused solely by changes in efficacy. Because none of the mutations in this study cause significant reductions in $I_{max\text{-}GABA}$ and the shifts in EC_{50} values range from 70-fold (R207C) to 18,000-fold (Y205C), it is clear that the in-

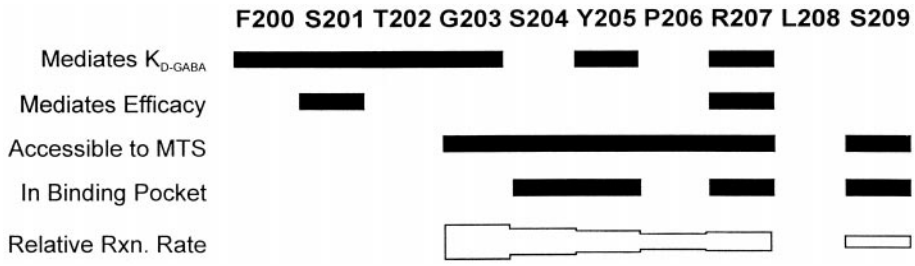

Figure 6. Graphic summary of results. *Bars* indicate which residues fall into each of the following categories: *Mediates $K_{D\text{-}GABA}$*, mutation of this residue alters microscopic affinity for GABA; *Mediates Efficacy*, mutation of this residue reduces efficacy of P4S; *Accessible to MTS*, we can detect reaction of MTSEA-biotin with a cysteine introduced at this position; *In Binding Pocket*, the rate at which MTSEA-biotin reacts with a cysteine introduced at this residue is slowed by the presence of both GABA and SR-95531. *Relative Rxn. Rate*, The height of the *bar* is scaled to the log of k_2 for each mutant with MTSEA-biotin.

creases in $EC_{50\text{-}GABA}$ values reflect, at least in part, a reduction in ligand affinity (K_D) at the GABA binding site. Although I_{max} comparisons between different mutant receptors are problematic because of poor control of expression levels, we feel confident that we would detect a >99% reduction in $I_{max\text{-}GABA}$. Moreover, five of the six mutations that shift $EC_{50\text{-}GABA}$ (all except R207C) also significantly reduce affinity for SR-95531, further suggesting that mutation of F200, S201, T202, G203, Y205, and R207 to cysteine alters the microscopic binding affinity of ligands at the GABA binding site.

When mutation of an amino acid disrupts agonist affinity, it has been used as evidence that the residue in question is located in the binding pocket. This, however, is not proof. Our result, that there is no detectable reaction of MTSEA-biotin with cysteines introduced at the positions F200–T202, suggests that these side chains are not facing into the water-accessible GABA binding pocket. Rather, these residues are likely to be buried in the protein or membrane lipid. Caution, however, must be taken with the interpretation of the accessibility results. The possibility that MTSEA-biotin modifies an introduced cysteine without affecting I_{GABA} must also be considered. However, it is unlikely that addition of the large biotin moiety would have no discernable affect on I_{GABA} if F200C, S201C, and T202C actually face into the binding pocket. Thus, although mutation of F200, S201, and T202 to cysteine results in large shifts in $EC_{50\text{-}GABA}$, we believe these residues are not lining the GABA binding pocket.

In contrast, the large shifts in $EC_{50\text{-}GABA}$ values caused by mutation of Y205 and R207 likely reflect disruptions of residues that line the binding site. Because MTSEA-biotin reacts with cysteines at positions S204, Y205, R207, and S209 and both GABA and SR95531 significantly slow their modification, we believe that these residues face into, and are part of, the GABA binding pocket.

In addition to reducing $K_{D\text{-}GABA}$, cysteine substitution at positions S201 or R207 also causes significant reductions in receptor efficacy. The fact that these mutations disrupt both agonist affinity and agonist efficacy suggests that this entire region may mediate local (i.e., in or near the binding pocket) allosteric transitions that translate agonist binding into channel opening.

Structure of the GABA binding pocket

Assessment of the accessibility of introduced cysteines to reaction with MTSEA-biotin reveals direct structural information about loop C of the GABA binding pocket. MTS reagents react 10^9–10^{10} times faster with ionized sulfhydryl groups than they do with protonated sulfhydryls (Roberts et al., 1986). Therefore, an introduced cysteine that reacts with an MTS reagent is likely to be oriented with its side chain in an aqueous environment in which ionization of the sulfhydryl is more probable (Pascual and Karlin, 1998).

Patterns of accessibility can be used to discern the secondary structure of a region. For example, after mutation to cysteine, alternating residues of the α_1 loop D domain are accessible to MTSEA-biotin, indicating that the region is a β-strand (Boileau et al., 1999). Here we show that six of seven sequential cysteine mutants in the β_2 loop C domain (G203C–R207C and S209C) are available for reaction with MTSEA-biotin. This accessibility pattern does not suggest a regular secondary structure, indicating that the region in question may be an extended coil or loop. This result agrees with secondary structure predictions for the N-terminal domain of the nACh receptor in which the loop C region is predicted to be a coil (Le Novère et al., 1999).

Additional structural information emerges from the rates at which the introduced cysteines react with MTSEA-biotin. Two main factors influence these rates: (1) ionization of the sulfhydryl side chain, which is more likely in an aqueous environment, and (2) steric hindrance (i.e., how difficult is it for the MTSEA-biotin molecule to physically approach and interact with the sulfhydryl group). The fast reaction rate measured for G203C ($k_2 \approx 250{,}000$ M^{-1} s^{-1}) indicates that the side chain of this residue is in an aqueous and sterically unrestricted environment such as would exist at the mouth of the binding pocket. The >2000-fold slower reaction rate measured for S209C ($k_2 \approx 120$ M^{-1} s^{-1}) indicates that the side chain of this residue is poorly ionized (in a relatively hydrophobic environment), located in a sterically confined region, or both. These are the conditions one might expect to find near the deepest point of the binding pocket. Significantly, the reaction rates for the introduced cysteines between G203 and S209 sequentially decline, almost continually, with progression along the peptide chain (Fig. 6, Table 2). This rate gradient is highly suggestive of a protein domain that traverses an aqueous pocket from its rim to its depths. This type of structure correlates with the water-filled tunnels in the nACh receptor identified by electron microscopy (Miyazawa et al., 1999). We hypothesize that, in the $GABA_A$ receptor, at least a portion of these tunnels lie at an α/β interface. The fact that none of the introduced cysteines before G203 appear to react with MTSEA-biotin suggests that the polypeptide chain may turn at this glycine (a residue that allows for maximum flexibility) and dive into the hydrophobic core of the protein or the lipid membrane.

Structural rearrangements involved in receptor gating

It has been speculated that the allosteric transition underlying gating of LGICs is primarily from quaternary rearrangements of the N-terminal domains of subunits with little change in tertiary or secondary structure (Corringer et al., 2000). The results presented here suggest that activation of the receptor involves movement of the α_1 and β_2 domains of the GABA binding site toward each other. Three residues that face into the binding pocket (S204, R207, and S209) experience reductions in accessibility to MTSEA-biotin during gating. This is exactly the result we would expect if convergence of two subunits were to decrease the vol-

ume of the binding pocket, making it more difficult for MTSEA-biotin to interact with residues in the pocket. Interestingly, GABA causes an increase in accessibility to MTSEA-biotin at position P206. We envision that P206C faces away from the binding pocket and, when GABA binds the area near P206, becomes more accessible to MTSEA-biotin.

Overall role of loop C in GABA binding and gating

Some of the results presented in this study are graphically summarized in Figure 6. This region appears to consist of two structurally distinct domains. The C-terminal residues of this domain (S204–S209) predominantly line the GABA binding pocket and are in an aqueous environment. The N-terminal residues (V199–T202) do not appear to be in an aqueous environment and thus are not part of the binding pocket. G203 seems to be a transition residue between these two domains in that it is easily modified by MTSEA-biotin (i.e., in an aqueous environment), but its modification is not slowed by GABA or SR95531 and thus does not seem to be facing into the binding pocket.

Functionally, the roles of the two structural domains seem to converge. The exquisite sensitivity of $K_{D\text{-}GABA}$ to perturbation of this entire region implies both domains are critically involved in maintaining the structural integrity of the binding pocket. Additionally, both domains contain residues (S201 and R207) that, when mutated to cysteine, cause reductions in agonist efficacy, implying that they may be part of the allosteric mechanism coupling binding to channel opening. The result that a cysteine introduced at position G203 experiences an environmental change in the presence of modulatory concentrations of pentobarbital indicates that the loop C region also responds to $GABA_A$ allosteric modulators. Finally, a role for this region in receptor gating is demonstrated by the fact that side chains at positions S204, R207, and S209 experience a change in environment concomitant with gating of the receptor. Thus, the loop C region of the GABA binding site contains dynamic elements that respond to both modulators and channel activation. The agonist-mediated binding site movements may be the initial trigger that drives channel opening.

REFERENCES

Akk G, Steinbach JH (2000) Activation and block of recombinant GABA(A) receptors by pentobarbitone: a single-channel study. Br J Pharmacol 130:249–258.

Amin J, Weiss DS (1993) GABAA receptor needs two homologous domains of the beta-subunit for activation by GABA but not by pentobarbital. Nature 366:565–569.

Anson LC, Chen PE, Wyllie DJA, Colquhoun D, Schoepfer R (1998) Identification of amino acid residues of the NR2A subunit that control glutamate potency in recombinant NR1/NR2A NMDA receptors. J Neurosci 18:581–589.

Basiry SS, Mendoza P, Lee PD, Raymond LA (1999) Agonist-induced changes in substituted cysteine accessibility reveal dynamic extracellular structure of M3–M4 loop of glutamate receptor GluR6. J Neurosci 19:644–652.

Boileau AJ, Kucken AM, Evers AR, Czajkowski C (1998) Molecular dissection of benzodiazepine binding and allosteric coupling using chimeric gamma-aminobutyric acidA receptor subunits. Mol Pharmacol 53:295–303.

Boileau AJ, Evers AR, Davis AF, Czajkowski C (1999) Mapping the agonist binding site of the $GABA_A$ receptor: evidence for a β-strand. J Neurosci 19:4847–4854.

Cheng Y, Prusoff WH (1973) Relationship between the inhibition constant (K1) and the concentration of inhibitor which causes 50 per cent inhibition (I50) of an enzymatic reaction. Biochem Pharmacol 22:3099–3108.

Chou T (1974) Relationships between inhibition constants and fractional inhibition in enzyme-catalyzed reactions with different numbers of reactants, different reaction mechanisms, and different types and mechanisms of inhibition. Mol Pharmacol 10:235–247.

Colquhoun D (1998) Binding, gating, affinity and efficacy: the interpretation of structure-activity relationships for agonists and of the effects of mutating receptors. Br J Pharmacol 125:924–947.

Corringer PJ, Le Novère N, Changeux JP (2000) Nicotinic receptors at the amino acid level. Annu Rev Pharmacol Toxicol 40:431–458.

Czajkowski C, Kaufmann C, Karlin A (1993) Negatively charged amino acid residues in the nicotinic receptor delta subunit that contribute to the binding of acetylcholine. Proc Natl Acad Sci USA 90:6285–6289.

del Castillo J, Katz B (1957) Interaction at endplate receptors between different choline derivatives. Proc R Soc Lond B Biol Sci 146:369–381.

Dennis M, Giraudat J, Kotzyba-Hibert F, Goeldner M, Hirth C, Chang JY, Lazure C, Chretien M, Changeux JP (1988) Amino acids of the *Torpedo marmorata* acetylcholine receptor alpha subunit labeled by a photoaffinity ligand for the acetylcholine binding site. Biochemistry 27:2346–2357.

Galzi JL, Changeux JP (1994) Neurotransmitter-gated ion channels as unconventional allosteric proteins. Curr Opin Struct Biol 4:554–565.

Ito T, Suzuki T, Wellman SE, Ho IK (1996) Pharmacology of barbiturate tolerance/dependence: GABAA receptors and molecular aspects. Life Sci 59:169–195.

Jackson MB, Lecar H, Mathers DA, Barker JL (1982) Single channel currents activated by γ-aminobutyric acid, muscimol, and (−)-pentobarbital in cultured mouse spinal neurons. J Neurosci 2:889–894.

Javitch JA, Fu D, Chen J, Karlin A (1995) Mapping the binding-site crevice of the dopamine D2 receptor by the substituted-cysteine accessibility method. Neuron 14:825–831.

Karlin A, Akabas MH (1998) Substituted-cysteine accessibility method. Methods Enzymol 293:123–145.

Krogsgaard-Larsen P, Falch E, Schousboe A, Curtis DR, Lodge D (1980) Piperidine-4-sulphonic acid, a new specific GABA agonist. J Neurochem 34:756–759.

Kucken AM, Wagner DA, Ward PR, Boileau JA, Czajkowski C (2000) Identification of benzodiazepine binding site residues in the gamma2 subunit of the gamma-aminobutyric acid(A) receptor. Mol Pharmacol 57:932–939.

Le Novère N, Corringer PJ, Changeux JP (1999) Improved secondary structure predictions for a nicotinic receptor subunit: incorporation of solvent accessibility and experimental data into a two-dimensional representation. Biophys J 76:2329–2345.

Liman ER, Tytgat J, Hess P (1992) Subunit stoichiometry of a mammalian K^+ channel determined by construction of multimeric cDNAs. Neuron 9:861–871.

Miyazawa A, Fujiyoshi Y, Stowell M, Unwin N (1999) Nicotinic acetylcholine receptor at 4.6 A resolution: transverse tunnels in the channel wall. J Mol Biol 288:765–786.

Ortells MO, Lunt GG (1995) Evolutionary history of the ligand-gated ion-channel superfamily of receptors. Trends Neurosci 18:121–127.

O'Shea SM, Wong LC, Harrison NL (2000) Propofol increases agonist efficacy at the GABA(A) receptor. Brain Res 852:344–348.

Pascual JM, Karlin A (1998) State-dependent accessibility and electrostatic potential in the channel of the acetylcholine receptor. Inferences from rates of reaction of thiosulfonates with substituted cysteines in the M2 segment of the alpha subunit. J Gen Physiol 111:717–739.

Roberts DD, Lewis SD, Ballou DP, Olson ST, Shafer JA (1986) Reactivity of small thiolate anions and cysteine-25 in papain toward methyl methanethiosulfonate. Biochemistry 25:5595–5601.

Robertson GA, Warmke JM, Ganetzky B (1996) Potassium currents expressed from *Drosophila* and mouse eag cDNAs in *Xenopus* oocytes. Neuropharmacology 35:841–850.

Sigel E, Baur R, Kellenberger S, Malherbe P (1992) Point mutations affecting antagonist affinity and agonist dependent gating of GABAA receptor channels. EMBO J 11:2017–2023.

Smith GB, Olsen RW (1994) Identification of a [^{3}H]muscimol photoaffinity substrate in the bovine gamma-aminobutyric acidA receptor alpha subunit. J Biol Chem 269:20380–20387.

Thompson SA, Whiting PJ, Wafford KA (1996) Barbiturate interactions at the human GABAA receptor: dependence on receptor subunit combination. Br J Pharmacol 117:521–527.

Uchida I, Cestari IN, Yang J (1996) The differential antagonism by bicuculline and SR95531 of pentobarbitone-induced currents in cultured hippocampal neurons. Eur J Pharmacol 307:89–96.

Ueno S, Bracamontes J, Zorumski C, Weiss DS, Steinbach JH (1997) Bicuculline and gabazine are allosteric inhibitors of channel opening of the $GABA_A$ receptor. J Neurosci 17:625–634.

Vandenberg RJ, Handford CA, Schofield PR (1992) Distinct agonist- and antagonist-binding sites on the glycine receptor. Neuron 9:491–496.

Westh-Hansen SE, Rasmussen PB, Hastrup S, Nabekura J, Noguchi K, Akaike N, Witt MR, Nielsen M (1997) Decreased agonist sensitivity of human GABA(A) receptors by an amino acid variant, isoleucine to valine, in the alpha1 subunit. Eur J Pharmacol 329:253–257.

Wilson GG, Karlin A (1998) The location of the gate in the acetylcholine receptor channel. Neuron 20:1269–1281.

Xu M, Akabas MH (1996) Identification of channel-lining residues in the M2 membrane-spanning segment of the GABA(A) receptor alpha1 subunit. J Gen Physiol 107:195–205.